Observation of the $\nu h_{11/2}$ sequence in the ^{97}Mo nucleus

D. Bucurescu, Ghe. Cătă-Danil, I. Cătă-Danil, M. Ivaşcu, N. Mărginean, and C. A. Ur
H. Hulubei National Institute of Physics and Nuclear Engineering, P.O. Box MG-6, Bucharest, Romania
(Received 5 July 2000; published 13 December 2000)

High-spin states have been studied in the ^{97}Mo nucleus with the reaction ^{82}Se(^{19}F,$p3n\gamma$) at 68 MeV. The main experimental result is the observation of the $\nu h_{11/2}$ quasiband structure up to the $31/2^-$ state at $E_x = 5.5$ MeV. The systematic behavior of this structure along the isotopic and isotonic sequences is presented. The structure of the ^{97}Mo is discussed in terms of the interacting boson-fermion model 1.

DOI: 10.1103/PhysRevC.63.014306 PACS number(s): 21.10.Hw, 23.20.En, 23.20.Lv, 27.60.+j

I. INTRODUCTION

Knowledge of the high-spin states in the $A \sim 100$ nuclei is more fragmentary than in many other nuclear regions. The Mo isotopes with N above 50 are, in particular, poorly studied at higher spins. Detailed knowledge from this point of view is rather worthwhile since these nuclei cover an interesting region with rather dramatic structural changes. Thus, at $N=60$ they experience one of the most abrupt known changes of deformation in the ground state, passing very suddenly from rather weakly deformed nuclei to nuclei with a large stable deformation [1]. Also, in the same region, a very interesting coexistence and competition between two different configurations was proposed almost 20 years ago [2].

The ^{97}Mo nucleus has not been studied until now with heavy-ion-induced reactions. Its low-energy, low-spin states are rather well known from β-decay work [3], as well as from many studies with light-particle-induced reactions, such as (d,p) [4], (p,d) [5], (n,γ) [6], and $(n,n'\gamma)$ [7] (for additional information, see the ENSDF adopted level scheme [8]). Information on higher-spin states in ^{97}Mo have been obtained with the $(\alpha,n\gamma)$ [9,10] and $(\alpha,3n\gamma)$ [10] reactions. As a result, positive-parity levels have been proposed up to a tentative $23/2^+$ state and those of negative parity up to a $15/2^-$ state [10].

The purpose of the present work has been to study the structure of the odd-A nucleus ^{97}Mo at higher spins, with the aid of a heavy-ion fusion-evaporation reaction. After presenting the experiments and their results, the structure of this nucleus is discussed in comparison with calculations based on the interacting boson-fermion model 1 (IBFM-1) and with level systematics in neighboring nuclei.

II. EXPERIMENTAL TECHNIQUES

The ^{97}Mo nucleus was populated and studied with the reaction ^{82}Se(^{19}F,$p3n\gamma$) at an incident energy of 68 MeV. The target was Se of thickness around 5 mg/cm^2 vacuum evaporated on a 2 mg/cm^2 Au foil, and having an enrichment of 92% in ^{82}Se. The $^{19}F^{8+}$ beam, of 68 MeV, was delivered by the Bucharest FN tandem van de Graaff accelerator. The experimental setup consisted of two intrinsic Ge detectors of 20% efficiency, a 1 liter NE213 scintillator detector placed in the forward direction for the detection of the neutrons, and one ΔE-E Si detector telescope for the identification of the charged particles. Details of the measurement geometries are specified in our recent work [14].

γ-γ, n-γ, and charged-particle-γ coincidences have been recorded on the hard disk of a PC and then analyzed offline. Different measurements have been performed. Thus, in a first run, γ-γ and charged-particle-γ coincidences were measured, the two Ge detectors being positioned at $\pm 125°$ with respect to the beam direction. Then, γ-γ and neutron-γ coincidences were measured; in one run, the two Ge detectors were kept in fixed positions, at 90° and $-45°$, respectively, while in another run one Ge detector was kept at $-145°$, and the other one was moved at the angles 15°, 35°, 45°, 55°, 75°, and 90°, respectively, thus covering an angular distribution measurement both in the singles and n-γ coincidence mode. The energy and efficiency calibrations were made with a ^{152}Eu source.

III. DATA ANALYSIS AND LEVEL SCHEME OF ^{97}Mo

The level scheme of ^{97}Mo, as evidenced in the present measurements, is shown in Fig. 1. The lower part of the positive-parity levels, as well as the first transition (565 keV) above the $11/2^-$ level at $E_x = 1.437$ MeV, were known from previous works [8–10] and have been confirmed in the present measurements. Starting from these known γ-ray transitions, the level scheme of Fig. 1 was constructed on the basis of γ-γ coincidence relationships observed in a symmetric matrix and γ-ray intensities. The assignment of all these transitions to ^{97}Mo has been confirmed by observing all of them in coincidence with both neutrons and protons, while they were absent in the coincidence with α particles. By comparing with transitions of the other observed reaction channels, as well as with calculations with the code CASCADE [15], it results that the $p3n$ channel was populated with an intensity of about 5% of the total fusion cross section (the calculated cross section for this channel is 28 mb). Table I gives a summary of the γ-ray transitions observed in ^{97}Mo and their properties and assignments.

Figure 2 is an example of a γ-ray spectrum gated by clean transitions (i.e., belonging only to ^{97}Mo), which shows the bandlike structure evidenced above the $11/2^-$ level (cf. Fig. 1). Gamma-ray intensities have been determined from the γ-ray spectrum registered at 55° in coincidence with the protons, with the exception of the transitions mentioned in the caption of Table I. This proton-gated spectrum, shown in Fig. 3, is dominated by transitions belonging to the

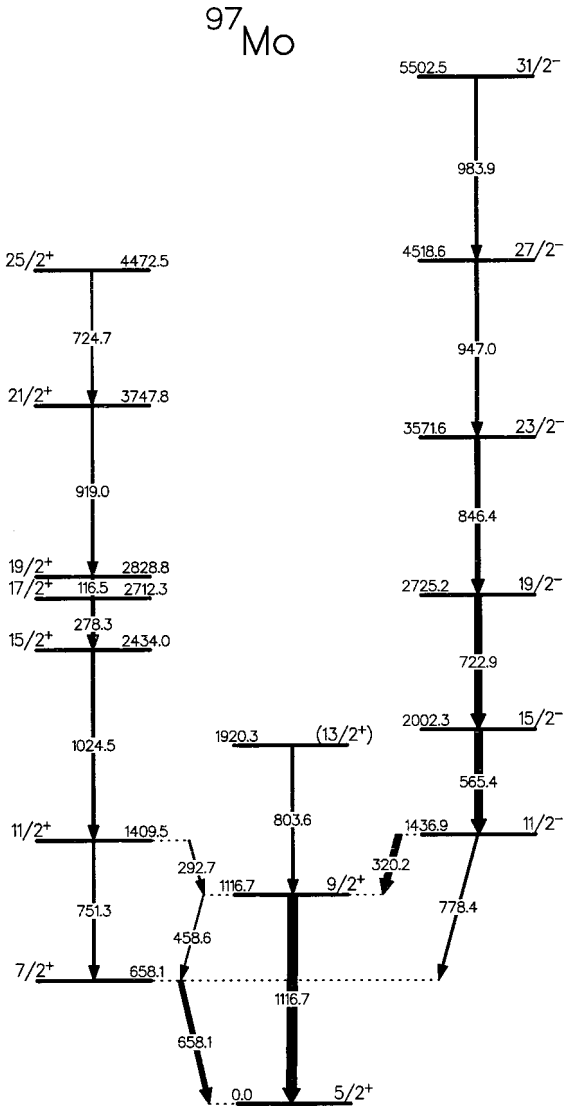

FIG. 1. Level scheme of ^{97}Mo as observed in the present measurements. For the level characteristics, see the discussion in text and Table I.

$p3n$ (^{97}Mo) and $p4n$ (^{96}Mo) channels, and some transitions from the $p5n$ (^{95}Mo) channel.

As mentioned, the level scheme of Fig. 1 coincides in the lower part with the one resulted from the (α,n) and $(\alpha,3n)$ experiments [9,10]. In the upper part of the positive-parity sequence we have reversed the order of the 116.5 keV and 278.3 keV transitions, confirmed the 919.0 keV transition (tentatively proposed in Ref. [10] above them), and added one more transition, of 724.7 keV.

As concerns the transitions placed above the $11/2^-$ state [10], we confirm the 722.9 keV γ-ray transition, but place it above the known 565.4 keV transition, while the other transitions from Fig. 1 are new. We have observed a few other weaker transitions (see spectrum of Fig. 2), obviously connected with the negative-parity sequence, but they could not be placed with certainty in the level scheme.

Information on the multipolarity of the γ-ray transitions in this level scheme has been obtained from both γ-ray angular distributions and directional correlation from oriented states (DCO) ratios, and are given in Table I. Clean angular distributions, which confirm the previously assigned multipolarities [9,10], could be obtained for some of the strongest transitions, such as 320.2, 565.4, and 1116.7 keV. Starting from these transitions, DCO ratios [16] have been determined for other transitions, from gates set on an asymmetric matrix, with the detector at 45° on one axis and the detector at 90° on the other axis. In this geometry the DCO ratio (R_{DCO}) for a dipole transition should be close to 0.5 when gating on a quadrupole transition and 1.0 when gating on a dipole transition, whereas a quadrupole transition is seen with a ratio of 1.0 when gating on another quadrupole and about 2.0 when gating on a dipole. Table I gives all these results, as well as the multipolarities assigned to different transitions. One can see that the sequence built above the $11/2^-$ state is made of quadrupole-type transitions; therefore we have assumed a sequence of $E2$ transitions up to spin $J=31/2$.

IV. DISCUSSION

A. Comparison with IBFM calculations

In this section we compare the existing experimental data to predictions of the interacting boson-fermion model 1 (IBFM-1) [17]. In this model the ^{97}Mo nucleus consists of a ^{96}Mo core, described by the interacting boson model 1 (IBM-1) [18], to which one couples an odd particle (fermion) allowed to occupy the single-particle orbitals from the valence space. In this model (''version 1'') one does not distinguish between neutrons and protons. In the present case this image might have, nevertheless, certain limitations. As noted in the Introduction, in the neutron-rich Mo isotopes the experimental data indicate a coexistence between two different configurations, whose mixing varies with N [2]. This situation could be successfully described [2] with an extension of the IBM in which a mixing between two different boson configurations is introduced [19], the physical meaning of it being the interplay between a ''normal'' configuration and the one resulting by breaking the existing (sub)shell closure through two-particle–two-hole ($2p$-$2h$) excitations. We note, however, that in ^{96}Mo the mixing between the ''basis'' [ground state (g.s.)] configuration and the ''intruder'' one is rather small, the lowest states being largely dominated by the ''normal'' (almost spherical) configuration [2]. We thus decided to treat the ^{96}Mo core, in a first approximation, with the simple IBM-1 model. In this way, the low (1.15 MeV) 0_2^+ state, which is largely due to the ''intruder'' $2p$-$2h$ configuration, will not be described; also, some details of the γ-ray decays of the excited states might be affected by neglecting this mixing. Thus, by using such a core in the IBFM description of ^{97}Mo, it is possible that certain low-lying experimental states cannot be correctly described. A comparison of such a simple approach to the low-excitation-energy experimental data is, nevertheless, interesting, in order to evidence possible ''intruder'' states in the odd-mass nucleus.

TABLE I. Properties of γ-ray transitions in ^{97}Mo, as observed in the ^{82}Se(^{19}F,$p3n$) reaction at 68 MeV. Legendre polynomial coefficients are determined from angular distributions measured in coincidence with neutrons. The DCO ratios (R_{DCO}) are determined from an asymmetric γ-γ coincidence matrix with one of the detectors at 90° and the other at 45°, the gated transition(s) being of quadrupole type, except for the cases marked with an asterisk when the gate was set on dipole transition(s). Gamma-ray intensities are from the spectrum at 55° measured in coincidence with protons, except for the 778.4, 846.4, and 947.0 keV transitions (contaminated with transitions in ^{96}Mo [24]) which were estimated from gates on the symmetric γ-γ matrix.

E_γ (keV)	I_γ (rel. units)	a_2/a_0	a_4/a_0	R_{DCO}	Multipolarity	Assignment E_i (keV)	E_f (keV)	$J_i^{\pi_i} \rightarrow J_f^{\pi_f}$
116.5	18.8(15)	−0.06(5)	−0.12(6)		D	2828.8	2712.3	$19/2^+ \rightarrow 17/2^+$
278.3	33.9(17)			0.45(12)	D	2712.3	2434.0	$17/2^+ \rightarrow 15/2^+$
292.7	14.3(11)					1409.5	1116.7	$11/2^+ \rightarrow 9/2^+$
320.2	65.4(23)	−0.45(11)	0.05(14)	0.57(6)	D	1436.9	1116.7	$11/2^- \rightarrow 9/2^+$
458.6	5.0(20)					1116.7	658.1	$9/2^+ \rightarrow 7/2^+$
565.4	74.9(30)	0.35(5)	−0.10(6)	1.80(24)*	Q	2002.3	1436.9	$15/2^- \rightarrow 11/2^-$
658.1	46.9(24)			0.50(11)	D	658.1	0	$7/2^+ \rightarrow 5/2^+$
722.9	69.9(45)			1.06(16)	Q	2725.2	2002.3	$19/2^- \rightarrow 15/2^-$
724.7	15.5(36)			2.3(7)*	Q	4472.5	3747.8	$25/2^+ \rightarrow 21/2^+$
751.3	22.9(18)			2.0(4)*	Q	1409.5	658.1	$11/2^+ \rightarrow 7/2^+$
778.4	15.7(38)					1436.9	658.1	$11/2^- \rightarrow 7/2^+$
803.6	25.7(45)				Q [a]	1921.0	1116.7	$(13/2^+) \rightarrow 9/2^+$
846.4	46.8(50)			0.87(18)	Q	3571.6	2725.2	$23/2^- \rightarrow 19/2^-$
919.0	20.3(26)			1.20(25)*	D	3747.8	2828.8	$(21/2^+) \rightarrow 19/2^+$
947.0	31.0(29)			0.88(17)	Q	4518.6	3571.6	$27/2^- \rightarrow 23/2^-$
983.9	23.4(30)			0.87(26)	Q	5502.5	4518.6	$31/2^- \rightarrow 27/2^-$
1024.5	27.2(39)			2.4(4)*	Q	2434.0	1409.5	$15/2^+ \rightarrow 11/2^+$
1116.7	100(5)	0.50(6)	−0.06(8)	1.70(27)*	Q	1116.7	0	$9/2^+ \rightarrow 5/2^+$

[a]From Ref. [10].

First, the ^{96}Mo core has been described with the IBM-1 model as a system of six bosons (the bosons have been counted with respect to the closed shell 50). The calculations have been performed with the codes PHINT and FBEM [20]. A reasonable description of the level and γ-decay scheme [11] has been obtained for the ground state quasiband up to 6^+ and the γ quasiband up to the 5^+ state. The parameters used for the nonmultipole form of the Hamiltonian (as described in the input for the code PHINT [20]) were HBAR=0.78, $C_L(L=0,2,4)=-0.1,-0.1,0.0$, $F=0.05$, and $G=-0.05$,

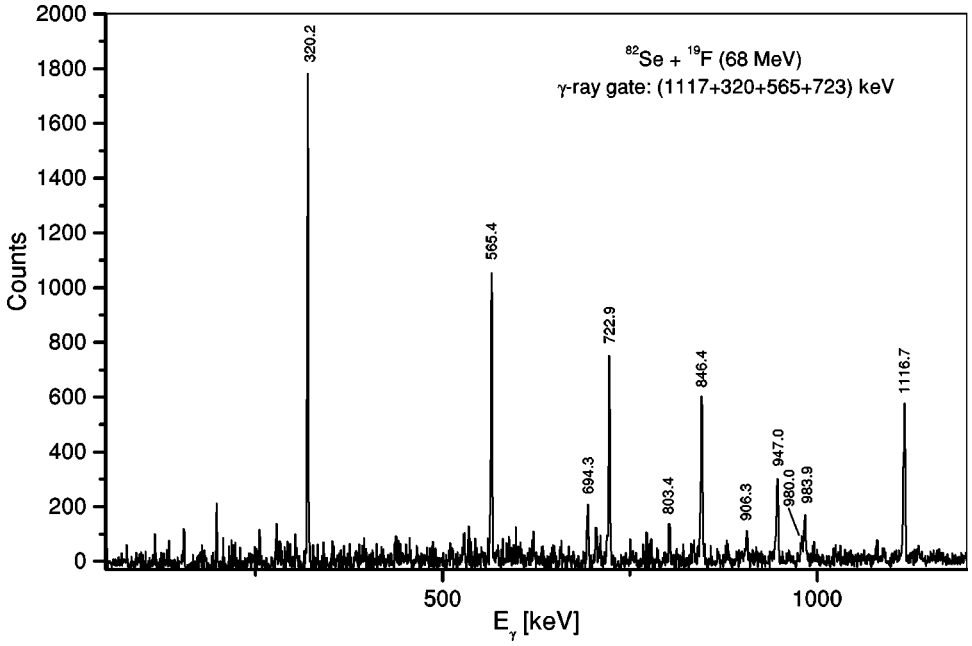

FIG. 2. Example of gated γ-ray spectrum obtained from a symmetric γ-γ coincidence matrix.

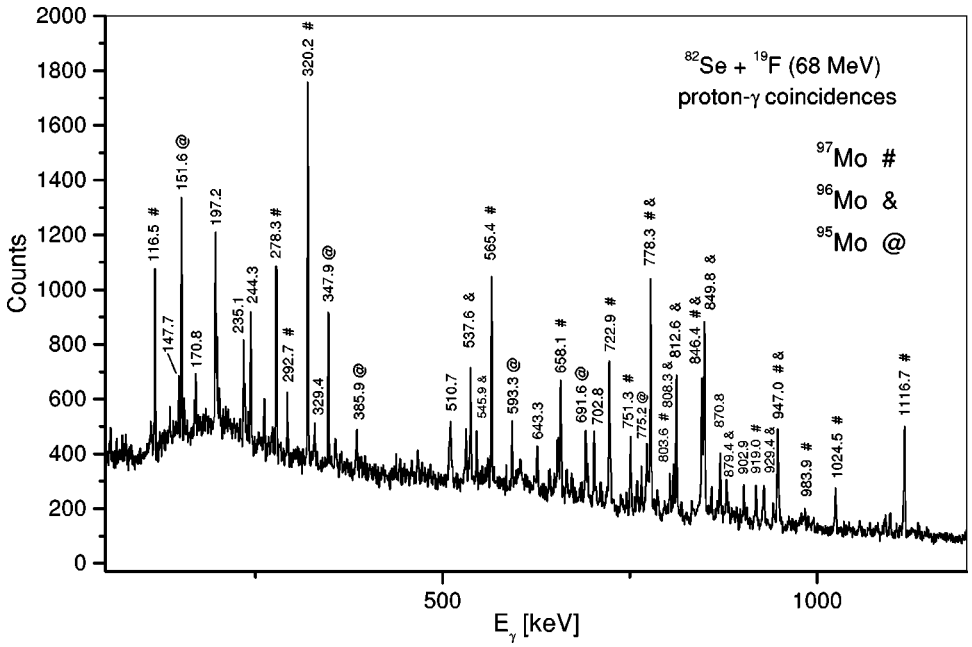

FIG. 3. γ-ray spectrum obtained in coincidence with protons. As indicated by labels, this spectrum is dominated by transitions from the $p3n$ (^{97}Mo), $p4n$ (^{96}Mo [11]), and $p5n$ (^{95}Mo [12]) channels. Some of the strongest, not labeled γ rays (such as, for example, 235 keV and 244 keV), belong to ^{92}Mo [13] and result from other Se isotopes in the target.

respectively (all in MeV).

Then, this core, which is rather close to the U(5) limit (anharmonic vibrator), has been used in the IBFM description of ^{97}Mo (see Fig. 4). The odd fermion was allowed to occupy all the orbitals from the 50 to 82 shell: $d_{5/2}, g_{7/2}$, $s_{1/2}, d_{3/2}, h_{11/2}$, and $f_{7/2}$ from the next major shell. The single-particle (s.p.) energies have been chosen according to the prescription of Reehal and Sorensen [21], only that of the $g_{7/2}$ orbital has been lowered by 0.2 MeV in order to improve the agreement with the data (see below). The quasiparticle energies and occupation probabilities have been calculated by using a simple BCS approach with a standard pairing gap of $12A^{-1/2}$ MeV. The calculations have been performed with the codes ODDA, PBEM, and SPEC, which calculate energy levels, $B(M1)$ and $B(E2)$ electromagnetic transition probabilities, and one-nucleon transfer spectroscopic factors, respectively [22]. The IBFM-1 Hamiltonian used is the standard one [17], in which, besides the IBM-1 Hamiltonian of the core and the quasiparticle energy term, there is a boson-fermion interaction with three terms: a monopole-monopole, a quadrupole-quadrupole, and an exchange interaction. We have given in Ref. [23] a detailed account of the particular parametrization used in these calculations both for this Hamiltonian and for the $M1$ and $E2$ electromagnetic transition operators.

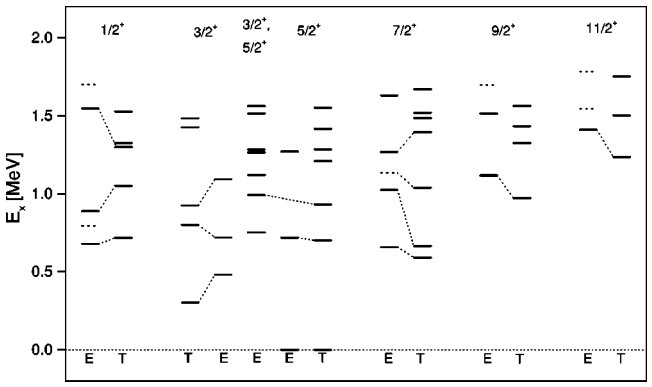

FIG. 4. Comparison of the low-spin energy levels of positive parity in ^{97}Mo with IBFM-1 predictions. Experimental and theoretical levels are marked by ''E'' and ''T,'' respectively. Experimental levels with tentative spin assignment [8] are drawn with dashed lines. The dotted lines connect experimental levels with the assigned theoretical levels (for details see text and Table II).

The Hamiltonian parameters (which are, essentially, the strengths of the three boson-fermion interaction terms) have been chosen by trying to describe as many spectroscopic quantities as possible. These included level positions, their γ-decay [branching ratios, and, when existing, absolute $B(E2)$ and $B(M1)$ probabilities], and one-neutron stripping spectroscopic factors. These parameters have been determined first for the positive-parity levels, for which there is quite extensive information [8]; in addition, in trying to reproduce the properties of the low-lying positive-parity states, one hopefully finds those parameters which produce the right mixing between the four positive-parity orbitals considered in the calculations. The values finally chosen for the strengths of the boson-fermion interactions are $A_0 = -0.15$ MeV, $\Gamma_0 = 0.2$ MeV, and $\Lambda_0 = 0.9$ MeV^2 (corresponding to the monopole, quadrupole, and exchange terms, respectively). The same parameters were able to provide a good description also for the negative-parity states; in order to obtain a more correct moment of inertia for the negative-parity band, only the A_0 value has been modified to -0.05 MeV. The influence of this parameter is mainly in the sense of a renormalization of the core state energies, while the mixing between the different orbitals remains essentially the same.

Figure 4 shows a comparison of the calculated positive-parity states of spin up to 11/2 with the known experimental levels. When the identification could be made unambiguously, the experimental level and its theoretical counterpart have been connected by a dotted line. This identification has

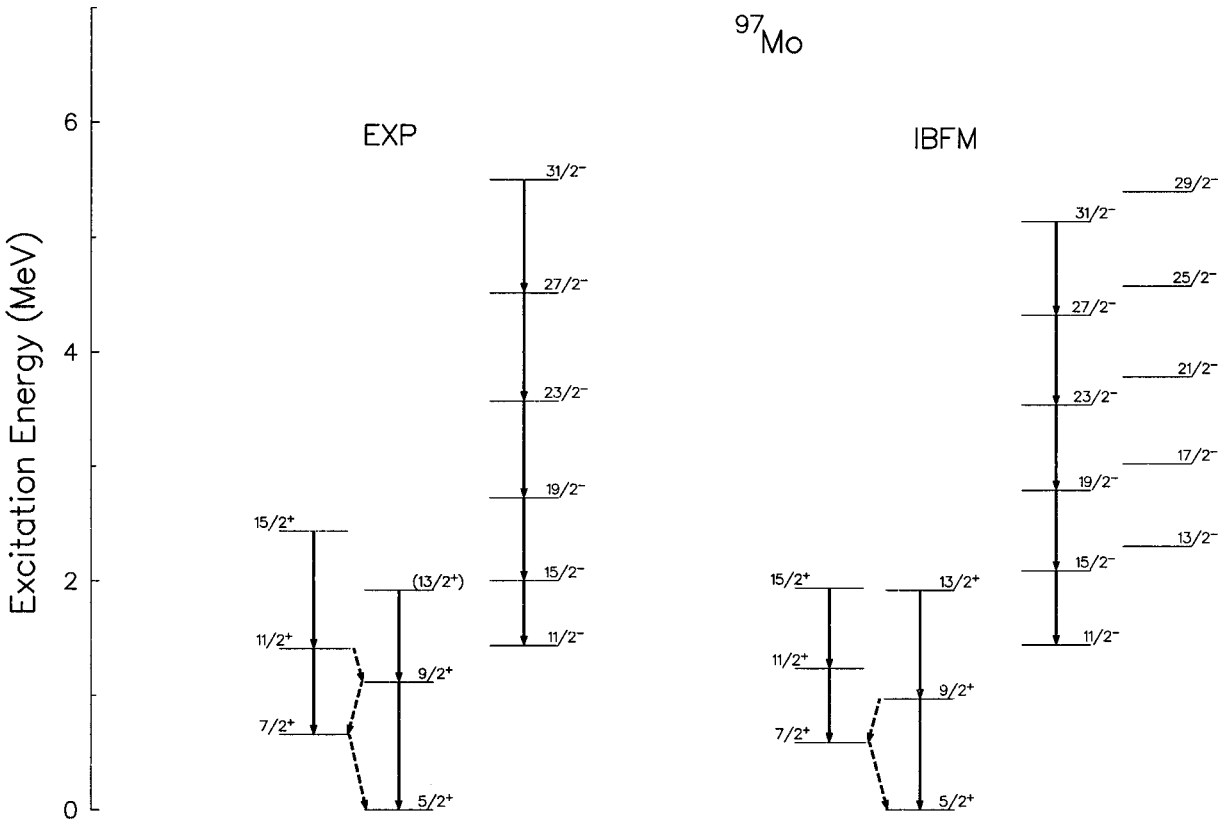

FIG. 5. Experimental and theoretical (IBFM-1) quasiband structures in ^{97}Mo. The calculated sequence $5/2^+,9/2^+,13/2^+$ is dominated by the $d_{5/2}$ orbital, whereas the $7/2^+,11/2^+,15/2^+$ is dominated by $g_{7/2}$ (see text). The configuration of the negative-parity band is mainly $h_{11/2}$ coupled to yrast core states. The predicted unfavored states $(13/2^-,17/2^-,\ldots)$ are also shown. The Hamiltonian used to calculate the negative-parity states is practically the same with the one used for the positive-parity states, and the excitation energy of the $11/2^-$ state relatively to the ground state $5/2^-$ is also well predicted. This figure shows only the main decays towards states of the same parity, with weaker branches represented by dashed lines.

been made on the basis of the level properties [energy, decay mode, spectroscopic factor in the (d,p) reaction]. One can see that up to about 1.2 MeV, an almost one-to-one correspondence could be established for all spin values. The picture of Fig. 4 is completed by Table II, in which the electromagnetic properties of these levels are shown, both the experimental and the calculated ones; branching ratios and, in most cases, also absolute transition probabilities are reasonably well reproduced.

The calculated configurations of these low-lying states are, in general, dominated by the $d_{5/2}$ and $g_{7/2}$ orbitals. Most of the lowest states have as main configuration a $d_{5/2}$ one, with the exception of the $7/2_1^+,11/2_1^+$, and $15/2_1^+$ states which are mainly due to the $g_{7/2}$ orbital. For the experimental $7/2_1^+$ state we had in competition two low-lying calculated states, one dominated by the $d_{5/2}$ and the other one dominated by the $g_{7/2}$ orbital. The choice of the appropriate configuration as ''$g_{7/2}$'' for this state was made on the basis of its large spectroscopic factor in the (d,p) reaction [4] and the rather low $B(E2)$ value of its transition towards the ground state (see Table I). To lower this state below the ''$d_{5/2}$'' one we had to modify the s.p. energy of the $g_{7/2}$ orbital with about 0.2 MeV relatively to the Reehal-Sorensen prescription, as remarked above. Figure 5 shows the experimental and calculated ''band'' structures. The $5/2_1^+,9/2_1^+,13/2_1^+$ sequence has as main configuration the $d_{5/2}$ shell coupled to core states, whereas the $7/2_1^+,11/2_1^+,15/2_1^+$ is based mainly on the $g_{7/2}$ shell. This situation is similar to that observed in the isotonic nucleus ^{101}Pd, and explained on the basis of a particle-plus-rotor model with a rather small deformation of the core ($\delta=0.12$) [24]. Above the $15/2^+$ state at 2.43 MeV, there is a change of structure which is no longer described by the IBFM, possibly an intersection with three-quasiparticle configurations.

As remarked above, for the description of the negative-parity states we have used the same boson-fermion interaction parameters (with the exception of a renormalization of the monopole term). The variation of the monopole-monopole interaction strength did not practically affect the relative position of the negative and positive states. From Fig. 5 one can see that the excitation energy of the $11/2^-$ state is reproduced rather correctly. The $E2$ band structure built on the $11/2^-$ state is also reasonably well described. The calculated states of spin 13/2, 17/2, 21/2, . . . are unfavored in energy (they are situated above the states of spin 15/2, 19/2, 23/2, . . . , respectively), and this explains why these states were not observed in the experiment. All these states have as dominant configuration the $h_{11/2}$ shell coupled to the yrast vibrational core states.

TABLE II. Electromagnetic properties of low-spin positive-parity levels in ^{97}Mo [8], compared to the IBFM predictions. Calculated branching ratios smaller than 1 (relative to 100, the standard value for the strongest branch) are given only if there is an experimental counterpart.

E_x (keV)	J_i^{π} [a]	J_i^{π} [b]	J_f^{π}	E_γ (keV)	$B(M1)$ (nm^2) Expt.	Calc.	$B(E2)$ (e^2 fm^4) Expt.	Calc.	Br. ratio (%) Expt.	Calc.
480.9	$3/2^+$	$3/2_1^+$	$5/2_1^+$	480.9	0.022(3)	0.0007	307(21)	602	100	100
658.1	$7/2^+$	$7/2_1^+$	$5/2_1^+$	658.1	0.068(36)	0.0002	$5.8^{+9.3}_{-5.0}$	54	100	100
679.6	$1/2^+$	$1/2_1^+$	$5/2_1^+$	679.6			135(11)	331	100	100
719.2	$5/2^+$	$5/2_2^+$	$3/2_1^+$	238.3	0.075(39)	0.234	<238	142	35(5)	44.7
			$5/2_1^+$	719.2	0.0064(34)	0.003	40(24)	445	100(5)	100
720.9	$3/2^+$	$3/2_2^+$	$5/2_1^+$	720.9	0.025^{+75}_{-11}	.027	27^{+82}_{-24}	3.2	100	100
888.2	$1/2^+$	$1/2_2^+$	$5/2_1^+$	888.2			53(24)	48.9	16(5)	8.8
			$3/2_1^+$	407.3		0.320		60.4	100(5)	100
			$1/2_1^+$	208.6		0.141		0.	-	5.9
			$3/2_2^+$	167.3		0.057		256	-	1.2
993	$3/2^+$,$5/2^+$	$5/2_3^+$	$5/2_1^+$	993		0.006		6.9		100
			$3/2_1^+$	512		10^{-6}		511		21.5
			$5/2_2^+$	274		0.0157		54.4		5.6
			$3/2_2^+$	272		0.141		45.1		48.3
1024.5	$7/2^+$	$7/2_2^+$	$5/2_1^+$	1024.5	0.050(13)	0.004	211(106)	573	100(3)	100
			$3/2_1^+$	543.6			74(26)	25	0.4(1)	0.2
			$7/2_1^+$	366.4		0.061		33.0	3.0(4)	6.0
			$5/2_2^+$	305.3		0.182		30.7	-	10.4
1092.6	$3/2^+$	$3/2_3^+$	$5/2_1^+$	1092.6	0.050(13)	0.108	53^{+82}_{-37}	4.8	100	100
			$3/2_1^+$	611.7		2×10^{-6}		97.8	11(2)	0.4
			$3/2_2^+$	371.7		0.075		2.8	-	1.6
1116.7	$9/2^+$	$9/2_1^+$	$5/2_1^+$	1116.7			265(20)	535	100(1)	100
			$7/2_1^+$	458.6		0.062		24.3	1.3(5)	9.2
			$5/2_2^+$	397.5			529(80)	10.0	1.15(14)	0.001
1268.6	$7/2^+$	$7/2_3^+$	$5/2_1^+$	1268.6		0.0015		2.0	100(5)	36.1
			$3/2_1^+$	787.7				464	35(5)	100
			$7/2_1^+$	610.5		0.0040		19.1	-	10.4
			$5/2_2^+$	549.4		0.0028		196	35(5)	11.7
			$5/2_3^+$	275.6		0.282		88.2	-	59.9
1409.6	$11/2^+$	$11/2_1^+$	$7/2_1^+$	751.5			>0.344	578	100	100
1515.7	$9/2^+$	$9/2_2^+$	$5/2_1^+$	1515.7			32(6)	12.1	100(5)	67.6
			$7/2_1^+$	857.6	0.0068(18)	2×10^{-5}	21(11)	308	28(5)	100
			$5/2_2^+$	796.5			159(79)	264	21(11)	59.2
			$7/2_2^+$	491.2		0.0004		163	-	3.7
			$9/2_1^+$	399.0		0.0456		4.4	-	28.8
			$7/2_3^+$	247.1		0.132		107	-	19.8
1920.3	$(13/2^+)$	$13/2_1^+$	$9/2_1^+$	803.6				739	100	100
			$11/2_1^+$	510.7		0.0275		11.8	-	21.2
2434.0	$15/2^+$	$15/2_1^+$	$11/2_1^+$	1024.4				951	100	100

[a]Adopted values from ENSDF (Ref. [8]).

[b]Assigned calculated state (comparison with the IBFM calculations).

B. Systematics of the $h_{11/2}$ structures in $A\sim100$ nuclei

We may try to follow the nuclear structure evolution in this mass region by examining the properties of the $h_{11/2}$ structure. Figure 6 shows its systematics both for the Mo isotopes with N larger than 50 and for the isotonic nuclei (with $N=55$). Among the neutron-rich Mo isotopes, ^{97}Mo is the only one where this structure is known at spins larger than 19/2. In the even-even Mo nuclei, it is known that the isotopes with $N\geqslant60$ become suddenly deformed [1]. The odd-A isotopes with $N=61$ and 63 show indeed a $h_{11/2}$ band with rotationlike characteristics. In ^{105}Mo ($N=63$) the unfavored states are also known, and their position with respect to the favored states, with a rather small signature splitting, indicates indeed a well-deformed band, with a deformation close to the axial symmetry. Right before $N=60$, in the $N=59$ isotope (^{101}Mo) the $h_{11/2}$ structure is not known, with

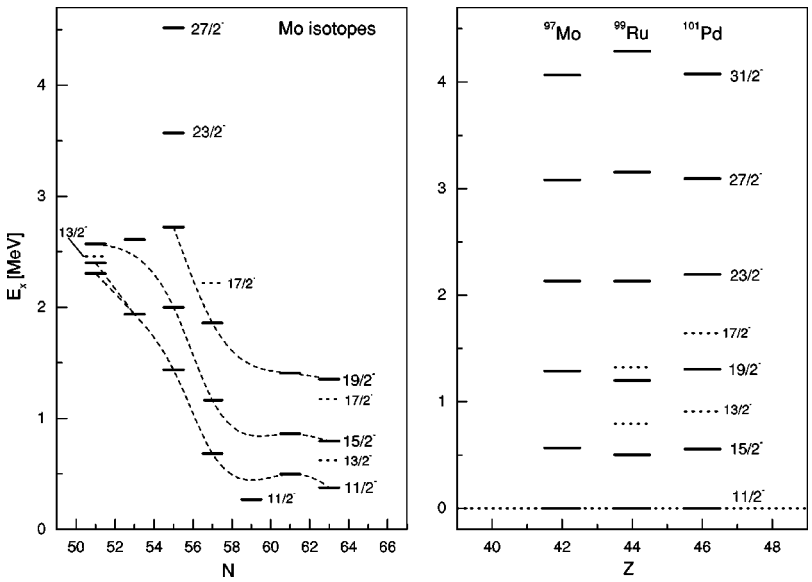

FIG. 6. Systematics of the $h_{11/2}$ sequences in the region close to ^{97}Mo. The left panel shows the evolution of this structure in the Mo isotopes with $N>50$. The known unfavored states are drawn with dotted lines. The dashed lines are spline fits through levels with the same spin; the $15/2^-$ level at $N=53$ and $11/2^-$ one at $N=59$ were not included in these fits. In the right panel, the sequence in ^{97}Mo is compared to that from the only isotonic ($N=55$) nuclei ^{99}Ru and ^{101}Pd in which it is known. Unfavored states are also drawn with a dashed line.

the exception of the ''bandhead'' $11/2^-$. In ^{99}Mo ($N=57$) one unfavored state is known ($17/2^-$), which shows an already reversed signature splitting, a situation which indicates a departure from the rotation alignment, and therefore a smaller deformation. In ^{97}Mo, although the unfavored states could not be determined, this trend probably continues (see also the IBFM prediction above). For the $N=53$ and 51 isotopes, not much is known, but due to the proximity of the $N=50$ shell closure, the $h_{11/2}$ structure in ^{93}Mo will probably no longer look like a quasiband.

In the right part of Fig. 6, the $h_{11/2}$ structure of ^{97}Mo is compared to that of other nuclei with $N=55$; only for ^{99}Ru [25] and ^{101}Pd [24] is this structure known. The ^{97}Mo structure is more similar to that of ^{101}Pd, whereas that in ^{99}Ru looks more rotational. In both ^{99}Ru and ^{101}Pd the known $13/2^-$ and $17/2^-$ states are unfavored in energy, a fact which strongly suggests a similar situation in ^{97}Mo, as discussed already above.

In ^{99}Ru the negative-parity structure could be determined up to rather high spins [25], and recently configuration terminations have been determined experimentally for both the negative- and positive-parity states [26], and the changes occurring along these bands have been interpreted within the cranking model. In the lowest part of these structures the nucleus is predicted with small deformation and rather γ soft [25,26]. In Fig. 7 we present the data from Fig. 6 in the form of experimental Routhians and alignments, which are more suggestive with respect to structural changes along the g.s. quasibands of the core nuclei and the $h_{11/2}$ structures in the odd-A nuclei. In all six nuclei we have used the same refer-

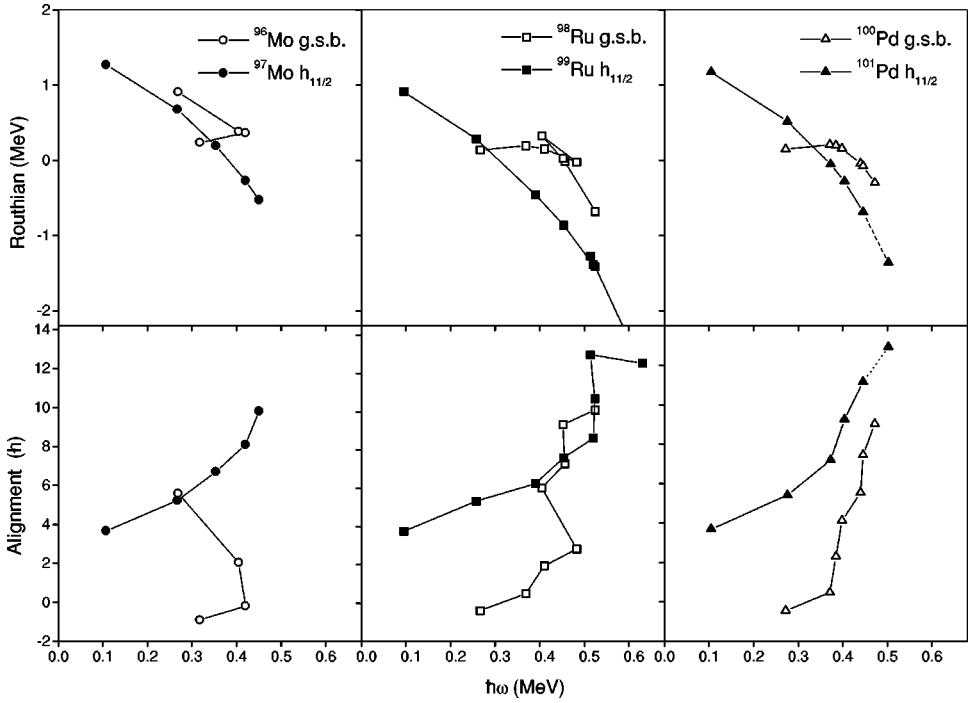

FIG. 7. Experimental Routhians and aligned angular momenta for the $N=55$ isotones and their even-even cores. A reference with Harris parameters $J_0=6.0\hbar^2$ MeV^{-1} and $J_1=15.7\hbar^4$ MeV^{-3} has been used.

ence (Harris parameters $J_0 = 6.0\hbar^2$ MeV^{-1} and $J_1 = 15.7\hbar^4$ MeV^{-3}) which has been determined from the ^{98}Ru nucleus. One should emphasize that for nuclei with small deformation and large γ softness the choice of a ''stable'' reference is questionable; nevertheless, we shall comment on the figures obtained in this way. In ^{98}Ru there is a crossing in the g.s. band at $\hbar\omega = 0.45$ MeV which has been attributed to the alignment of $h_{11/2}$ neutrons; the crossing seen in the $h_{11/2}$ band of ^{99}Ru at about $\hbar\omega = 0.5$ MeV has been attributed to the alignment of a pair of $g_{9/2}$ protons [25]. In the Mo and Pd isotopes from Fig. 7, the situation is less clear. In both ''cores'' ^{96}Mo and ^{100}Pd there is a drastic change of structure at $\hbar\omega \sim 0.4$ MeV or even less, probably an early $(h_{11/2})^2$ neutron alignment. The alignment gain in the $h_{11/2}$ structures in both ^{97}Mo and ^{101}Pd is rather smooth up to that frequency; then, the existing data in ^{97}Mo indicate the beginning of an upbending, while in ^{101}Pd a similar upbending is seen, which are probably due to the $g_{9/2}$ proton pair alignment.

V. CONCLUSIONS

This study reported for the first time a heavy-ion fusion-evaporation reaction approach to the high-spin states of ^{97}Mo. As a result, the positive-parity yrast structure has been extended up to a $25/2^+$ state, and the negative-parity states, consisting of a bandlike structure of quadrupole transitions built above the known $15/2^- \rightarrow 11/2^-$ one, have been observed up to the $31/2^-$ state.

Theoretical calculations for this nucleus have been performed within the multishell IBFM-1 approach. For both parities we have used practically the same Hamiltonian. In the positive-parity case, a one-to-one correspondence between the experimental and calculated levels could be made up to about 1.2 MeV excitation for all spins up to 11/2; the calculations describe also the beginnings of two bandlike structures based on the one-quasiparticle states $d_{5/2}$ and $g_{7/2}$. The excitation energy of the $11/2^-$ state is correctly predicted, and the observed quasiband structure above it is interpreted as the favored $h_{11/2}$ structure. A discussion of this structure is also presented in the context of the systematics of the $h_{11/2}$ states in the Mo isotopes with $N > 50$ and in the $N = 55$ isotones.

ACKNOWLEDGMENTS

We thank the Romanian National Agency for Science and Technology (ANSTI) for support from a research grant.

[1] *Nuclear Structure in the Zirconium Region*, edited by J. Eberth, R.A. Meyer, and K. Sistemich (Springer, New York, 1988).
[2] M. Sambataro and G. Molnar, Nucl. Phys. **A376**, 201 (1982).
[3] B. Singh, R.J. Coz, A.H. Kukoc, J.D. King, and H.W. Taylor, Nucl. Phys. **A129**, 104 (1969).
[4] L.R. Medsker and Y.L. Yntema, Phys. Rev. C **9**, 664 (1974).
[5] P.K. Bindal, D.H. Youngblood, R.L. Kozub, and P.H. Hoffmann-Pinther, Phys. Rev. C **12**, 390 (1975).
[6] K. Rimawi and R.E. Chrien, Phys. Rev. C **15**, 1271 (1977).
[7] U. Abbondanno, F. Demanins, and F. Raicich, Nuovo Cimento A **102**, 1533 (1989).
[8] A. Artna-Cohen, Nucl. Data Sheets **70**, 85 (1993), and the ENSDF database evaluated and updated by the Brookhaven National Laboratory.
[9] L. Mesko, A. Nilsson, S.A. Hjorth, M. Brenner, and O. Holmlund, Nucl. Phys. **A181**, 566 (1972).
[10] C.M. Lederer, J.M. Jaklevic, and J.M. Hollander, Nucl. Phys. **A169**, 489 (1971).
[11] C.M. Lederer, J.M. Jaklevic, and J.M. Hollander, Nucl. Phys. **A169**, 449 (1971).
[12] T.W. Burrows, Nucl. Data Sheets **68**, 635 (1993).
[13] C.M. Baglin, Nucl. Data Sheets **66**, 347 (1992).
[14] N. Mărginean, D. Bucurescu, Ghe. Căta-Danil, I. Căta-Danil, M. Ivaşcu, and C.A. Ur, Phys. Rev. C **62**, 034309 (2000).
[15] F. Pühlhofer, Nucl. Phys. **A280**, 267 (1977).
[16] K.S. Krane, R.M. Steffen, and R.M. Wheeler, Nucl. Data Tables **11**, 351 (1973).
[17] F. Iachello and O. Scholten, Phys. Rev. Lett. **43**, 679 (1979).
[18] A. Arima and F. Iachello, Ann. Phys. (N.Y.) **99**, 253 (1976); **11**, 201 (1978); Phys. Rev. Lett. **40**, 385 (1978).
[19] P.D. Duval and B.R. Barrett, Nucl. Phys. **A376**, 213 (1982).
[20] O. Scholten, computer codes PHINT and FBEM, KVI Report No. 63, 1979.
[21] B.S. Reehal and R.A. Sorensen, Phys. Rev. C **2**, 819 (1970).
[22] O. Scholten, computer codes ODDA and PBEM, KVI Internal Report No. 252, 1982; computer code SPEC (unpublished).
[23] M. Ivaşcu, N. Mărginean, D. Bucurescu, I. Căta-Danil, C.A. Ur, and Yu.N. Lobach, Phys. Rev. C **60**, 024302 (1999).
[24] R. Popli, F.A. Rickey, and P.C. Simms, Phys. Rev. C **22**, 1121 (1980).
[25] J. Gizon, D. Jerrestam, A. Gizon, M. Jozsa, R. Bark, B. Fogelberg, E. Ideguchi, W. Klamra, Th. Lindblad, S. Mitarai, J. Nyberg, M. Piiparinen, and G. Sletten, Z. Phys. A **345**, 335 (1993).
[26] J. Gizon (private communication); J. Timar *et al.*, Phys. Rev. C **62**, 044317 (2000).